Research Square

Preprints are preliminary reports that have not undergone peer review.
They should not be considered conclusive, used to inform clinical practice,
or referenced by the media as validated information.

Microstructure and mechanical properties of W/CuCrZr joints brazed using a CoFeCrNiCuSn high-entropy alloy filler

Rui Zhang

zr200205@163.com

Anhui Polytechnic University

Gang Wang

Anhui Polytechnic University

Yinhe Zeng

Anhui Polytechnic University

Wei Wang

Anhui Technical College of Mechanical and Electrical Engineering

Yu Zhao

Anhui Polytechnic University

Rujie He

Beijing Institute of Technology

Caiwang Tan

Harbin Institute of Technology

Research Article

Keywords: High entropy alloy, W, CuCrZr, Brazing, Shear strength

Posted Date: November 23rd, 2026

DOI: https://doi.org/10.21203/rs.3.rs-11206118/v1

License: This work is licensed under a Creative Commons Attribution 4.0 International License.
Read Full License

Microstructure and mechanical properties of W/CuCrZr joints brazed using a CoFeCrNiCuSn high-entropy alloy filler

Rui Zhang[a], Gang Wang[a, b*], Yinhe Zeng[a], Wei Wang[c], Yu Zhao[a], Rujie He[d], Caiwang Tan[e]

a *Anhui Key Laboratory of High-performance Non-Ferrous Metal Materials, Anhui Polytechnic University, Wuhu 241000, China*

b *Key Laboratory of Additive Manufacturing (3D Printing) of Anhui Province, Wuhu 241000, China*

c *School of Aviation and Materials, Anhui Technical College of Mechanical and Electrical Engineering, Wuhu 241000, China*

d *Institute of Advanced Structure Technology, Beijing Institute of Technology, Beijing 100081, China*

e *State Key Laboratory of Advanced Welding and Joining, Harbin Institute of Technology, Harbin 150001, China*

Corresponding author: Gang Wang(gangwang@ahpu.edu.cn)

ABSTRACT:

A CoFeCrNiCuSn high-entropy alloy is employed as the filler metal for brazing W to CuCrZr alloy. The impact of brazing temperature and holding duration on the microstructure, phase composition, and shear strength of the brazed joint is examined. SEM and TEM are used to characterize the microstructure, while EDS analyzes the phase composition. The experimental findings indicate that the joint's microstructure primarily consists of FCC, BCC, Cu (s, s), and Cu_3Sn. The characteristics of CuCrZr/CoFeCrNiCuSn/W joints are primarily influenced by the extent of interfacial

reactions, the width of the weld and the proportion and distribution of FCC/Cu_3Sn phases. The optimal brazing condition is determined to be 1000 °C for 20 min, under which the joint exhibited a maximum shear strength of 247 MPa.

Keywords: High entropy alloy; W; CuCrZr; Brazing; Shear strength

1. Introduction

Tungsten (W) and CuCrZr are the key candidate materials for high-heat-flux components and heat-sink components, respectively [1, 2]. Tungsten (W) has the characteristics of high melting point, high hardness but high brittleness, while CuCrZr alloy has excellent thermal conductivity and good plasticity, and the two exhibit significantly different physical and chemical properties [3, 4]. At present, the connection of W and Cu alloy mainly use traditional fillers for vacuum brazing or diffusion welding, and the joint strength is low [5-7]. Conventional fillers, such as Ag-Cu-based, Ni-based and Cu-Mn-based, form intermetallic compounds (IMC) when reacting with W or Cu, which become the weak points in the joint [8-11].

High-entropy alloy fillers can effectively enhance joint strength compared to traditional fillers [12, 13]. Luo et al. successfully brazed SiC ceramics to Zr using a CoCrFeNiCuSn high-entropy alloy (HEA) filler. The resulting joint was mainly composed of $Zr(Fe, Cr)_2$ Laves phase, Zr_2Cu, α-Zr solid solution, (Zr, Sn) phase, and residual HEA phase. The joint exhibited shear strengths of 221 MPa at room temperature and 207 MPa at 600 °C, respectively. These values were significantly higher than those obtained using a conventional Ag-Cu-Ti filler metal, demonstrating

the promising potential of the HEA filler for maintaining joint strength at elevated temperatures[14]. Yang et al. employed CoFeNiCrCu HEA to join ZrB_2-SiC ceramics with Nb, and the joint strength remained 94 MPa at 650 °C, reflecting good thermal stability [15]. Research on the use of high-entropy alloys as filler metals for joining similar and dissimilar metallic materials has also attracted increasing attention [16, 17]. Meng et al. employed a CrFeCoNiCu high-entropy alloy (HEA) interlayer to diffusion bond a tungsten alloy to steel. The joint achieved a maximum tensile strength of 592 MPa after bonding at 950 °C for 1 h [18]. This provides strong evidence for the application of HEA filler in alloy joining.

At present, studies on the joining of W/CuCrZr using HEA fillers remain limited. Therefore, in this study, a CoFeCrNiCuSn HEA filler is introduced for joining W to CuCrZr. The multicomponent nature of the HEA filler is expected to promote the formation of solid-solution phases and potentially suppress the formation of excessive brittle intermetallic compounds during brazing. The mechanical properties and microstructure of CuCrZr/CoFeCrNiCuSn/W joints are studied by vacuum brazing CuCrZr and W. Furthermore, a systematic analysis is conducted on how brazing temperature and holding time affect the mechanical and interfacial microstructure performance of the joints.

2. Experimental

Tungsten (W) (purity = 99.95 wt.%, CTE = 4.5×10^{-6} K^{-1}, density = 19.35 g/cm³) was offered by Beijing Runzhijiaobo Metal Materials Co., Ltd. The CuCrZr alloy (CTE

= 17.0 × 10^{-6} K^{-1}, density = 8.9 g/cm³) was procured from Changsha Tianjiu Metal Materials Co., Ltd. The CoFeCrNiCuSn HEA alloy ingot was created by vacuum arc melting a blend of Co, Fe, Cr, Ni, Cu and Sn, each having a purity greater than 99.95%. The XRD pattern of the CoFeCrNiCuSn HEA filler is shown in Fig. 1 a). According to our previous study [14], its melting temperature is approximately 997 °C.

Prior to brazing, W and CuCrZr were cut into 4mm × 4mm × 4mm and 10mm × 10mm × 4mm by electric spark wire cutting machine. CoFeCrNiCuSn HEA ingot was converted into a sample sized 4mm × 4mm × 4mm. The CoFeCrNiCuSn HEA ingot was processed into a sample with a size of 4mm × 4mm × 4mm. W and CuCrZr samples were polished by SiC sandpaper (400 # - 2000 #) to remove the surface oxide layer. CoCrFeNiCuSn HEA was processed into 400μm alloy foil by diamond machine for wire cutting. The alloy foils were subsequently ground with SiC abrasive papers to reduce their thickness to approximately 200 μm. Subsequently, all samples were ultrasonically cleaned in ethanol for 10 min. Fig. 1 b) illustrates the assembly structure of the brazed sample, with the base metal and HEA filler arranged from top to bottom as W/CoFeCrNiCuSn/CuCrZr. To examine the effect of different brazing temperatures on joint properties, the joints were subjected to brazing at 980 °C, 990 °C, 1000 °C, 1010 °C, and 1020 °C for 15 minutes. According to the experimental results, the optimum brazing temperature was determined to be 1000 °C. Brazing experiments were then performed at 1000 °C for 10, 15, 20, and 25 minutes to investigate the impact of holding time on joint characteristics. The brazing experiment was carried out in SML1550 vacuum brazing furnace without external pressure, and the vacuum level was

kept below 1×10^{-3} Pa during the whole experiment. The brazing process is shown in Fig. 1 c). The brazing temperature was increased from room temperature to the target level at a rate of 10 °C/min during the heating stage. Two pronounced outgassing peaks were observed at approximately 400 and 800 °C for the CuCrZr alloy. During the heating process, the CuCrZr alloy was kept at these two temperatures for 15 minutes respectively to promote gas release [19]. During the cooling phase, the temperature decreased to 500 °C at a speed of 5 °C per minute, after which the sample was cooled to room temperature within the furnace.

After brazing, the samples were cut using a diamond wire cutting machine. Subsequently, the samples after cutting were cold mounted, polished and cleaned for subsequent testing. The joints' microstructure was analyzed using scanning electron microscopy (SEM, TESCAN MIRA4) and energy dispersive spectroscopy (EDS). The joint's phase composition was analyzed using a micro-area X-ray diffractometer (XRD, D-MAX Rapid II) and a transmission electron microscope (TEM, Tecnai F20, FEI). The micro-area X-ray diffractometer was used for phase analysis, the scanning angle (2θ) was 5° - 90°, and the scanning speed was 5°/min. As shown in Fig. 1 d), the brazing samples were fixed in the designed fixture and the shear properties of the joints were tested by Instron 5500 universal material testing machine. The loading rate was constant at 5 N/s. The average value was determined from four shear tests performed with different brazing parameters.

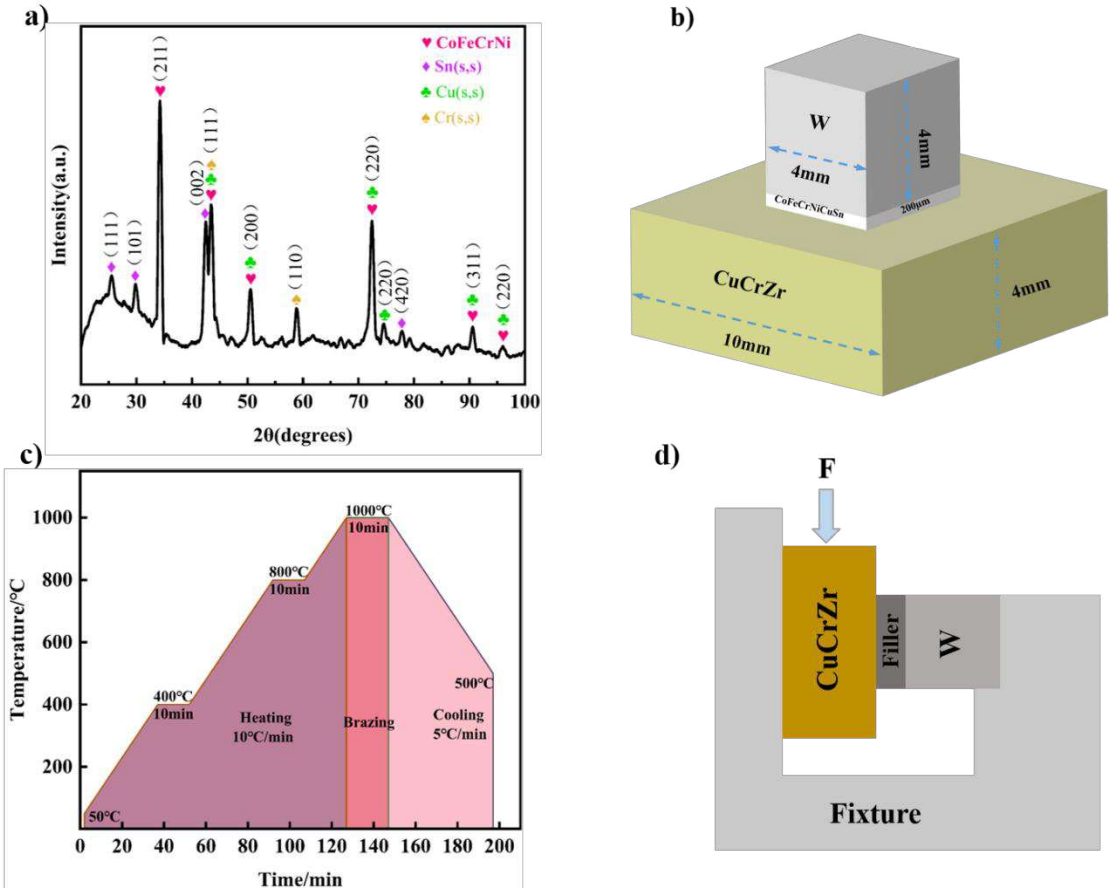


Fig. 1. a) XRD patterns of the CoFeCrNiCuSn filler. b) Schematic illustration of the vacuum brazing assembly. c) Brazing process diagram. d) Shear test die.

3. Results and discussion

As shown in Fig. 2, the microstructure and element distribution of the CuCrZr/CoFeCrNiCuSn/W joint brazed at 1000 °C for 20 minutes reveal no significant defects such as pores or cracks, indicating effective brazeability between CuCrZr, W, and the CoFeCrNiCuSn filler. As shown in Fig. 2 a), there are three areas marked on the joint for convenience. The CuCrZr side, joint center, and W side are referred to as zones I, II, and III, respectively. Zones I and II showed complete metallurgical fusion. The boundary between zones II and III is clear. Fig. 2 b) to i) illustrate the distribution of elements within the brazed joint. Cu, Ni, Co and Sn are mainly distributed in zones

I and II. W is mainly distributed in zone III. Zr, as a minor alloying element in CuCrZr, was mainly detected in the CuCrZr side. A small amount of Zr was also detected on the W side, indicating that Zr diffused from CuCrZr toward the brazing seam and W side during vacuum brazing.

Fig. 3 a) is overall view of the joint at 1000 °C for 20 min. Fig. 3 b) and c) illustrate enlarged views of zone II and the connection between zones II and III. Fig.3 b) and c) show that zone II at the joint is mainly composed of A, B, C and D phases. EDS was used to analyze the phase composition at the joint, with the findings presented in Table 1. In the A phase, the molar ratio of Cu and Sn is about 3 : 1, which is presumed to be Cu_3Sn. The B phase primarily consists of Cu, which is believed to match the Cu (s, s) phase. The reason is that the combination of Cu and other elements is weak, which is more prone to intergranular segregation and the formation of Cu (s, s) phase [20-22]. In phase C, the atomic ratio of Cr, Fe, Co, and Ni is approximately 1:1:1:1, suggesting that this phase may correspond to an FCC solid-solution phase. The content of W and Cr in D phase is higher, which is speculated to be BCC phase.

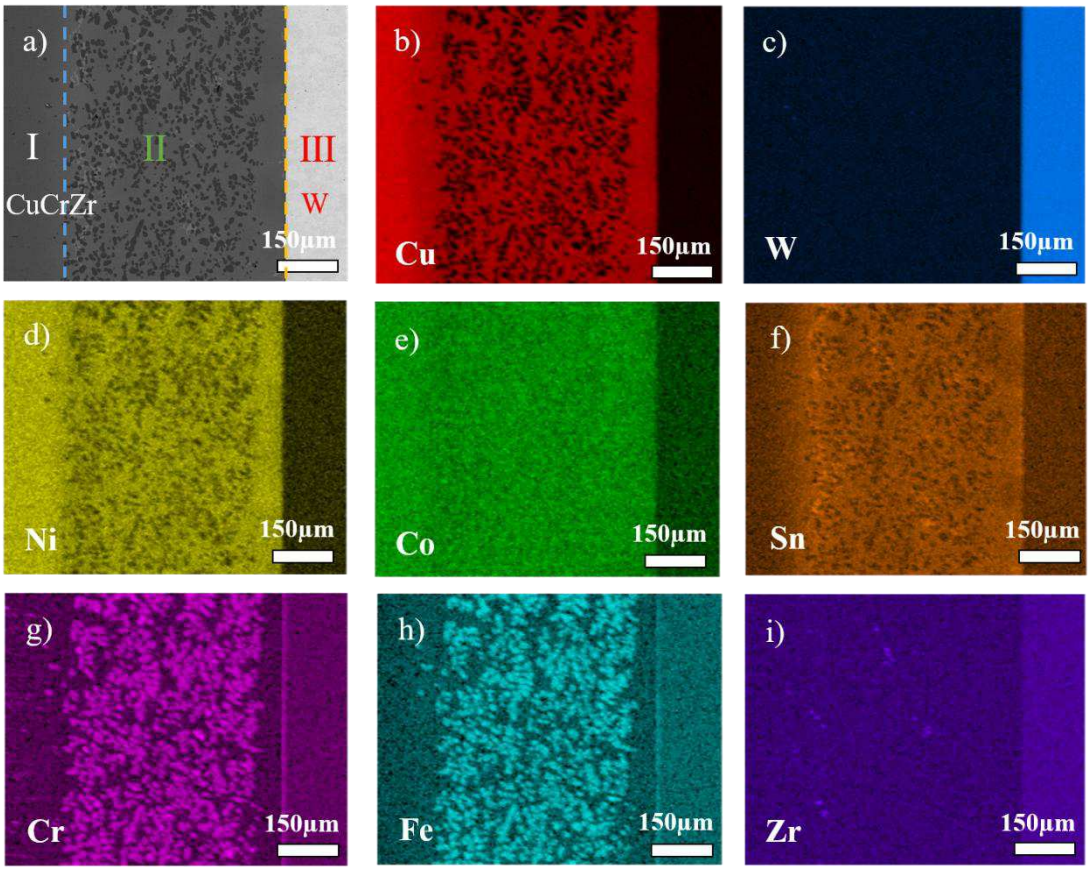


Fig. 2. Microstructure and energy spectrum analysis of CoCrFeNiCuSn brazing joint.

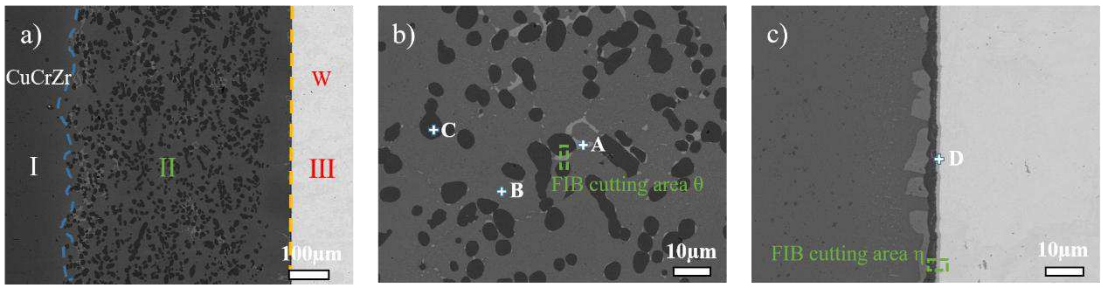


Fig. 3. SEM images of CuCrZr/W joint joined by CoFeCrNiCuSn filler at 1000℃ for 20 min.

Table 1 Elemental compositions and possible phases in regions A-D in Fig. 3 (at.%).

Position	Cr	Fe	Co	Ni	Cu	Zr	Sn	W	Possible Phase
A	1.11	1.40	1.51	13.57	59.40	0.13	22.82	0.07	Cu_3Sn
B	0.26	0.32	0.83	3.35	88.81	0.21	6.16	0.06	Cu(s, s)
C	29.77	28.63	26.84	10.51	3.49	0.00	0.60	0.16	FCC
D	25.41	15.52	19.16	2.97	0.37	1.28	0.13	35.16	BCC

The phases in the joints are characterized by TEM and SAED. The selected regions θ and η in Fig. 3 a) are prepared using a focused ion beam (FIB) system and subsequently analyzed. The transmission electron microscope bright field (BF) image

of the θ region in the joint is presented in Fig. 4 a). Fig. 4 b) - i) shows the EDS mappings from Fig. 4 a). The SAED patterns are shown in Fig. 5 b) and c). Regions a and c in Fig. 4 a) are mainly composed of Co, Fe, Cr and Ni elements, which are identified as FCC phase by SAED analysis. Region b mainly contains Cu and Sn elements, and it is determined to be a Cu_3Sn intermetallic compound (IMC) by SAED analysis. Fig. 5 d) - g) show the BF image of the transmission electron microscope and the corresponding SAED pattern in the η region of the joint. The d region is Cu (s, s) phase. The e region is FCC phase. The f region contains more W elements, which is confirmed as the BCC phase by SAED analysis.

The phase composition in the joint is further determined by analyzing the interfacial reaction layer with micro-area XRD, as illustrated in Fig. 6. The main phases of CuCrZr/W joints brazed with CoFeCrNiCuSn filler are FCC, Cu_3Sn, Cu (s, s) and BCC, which are consistent with the results of EDS and TEM analysis. Therefore, the joint's phase structure is defined as Cu (s, s) + Cu_3Sn + FCC + BCC.

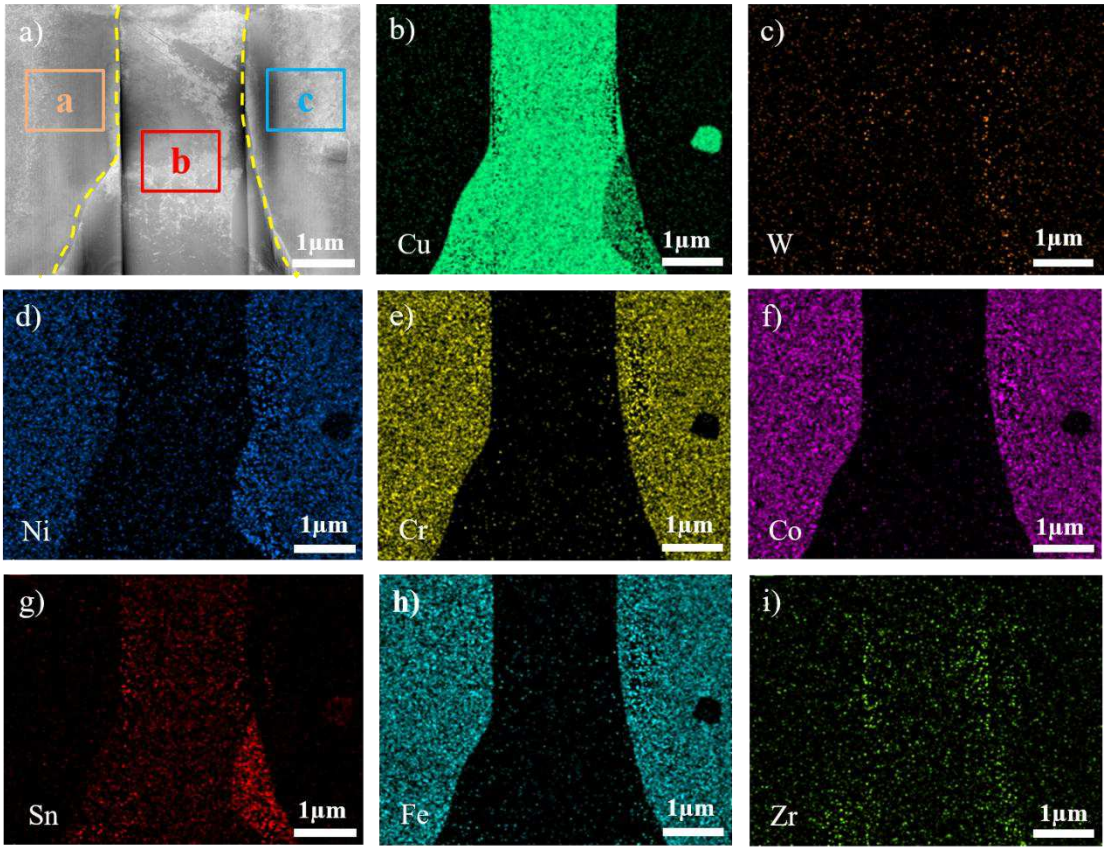


Fig. 4. TEM BF image and elemental maps of the W/CuCrZr brazed joint interface.

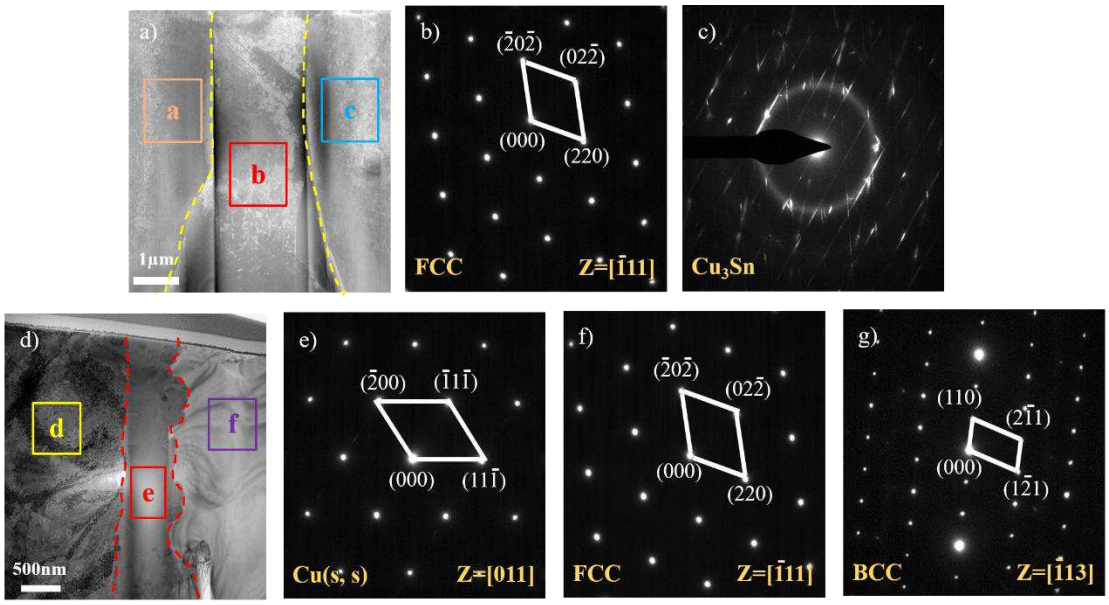


Fig. 5. TEM BF image of the grains and SAED patterns.

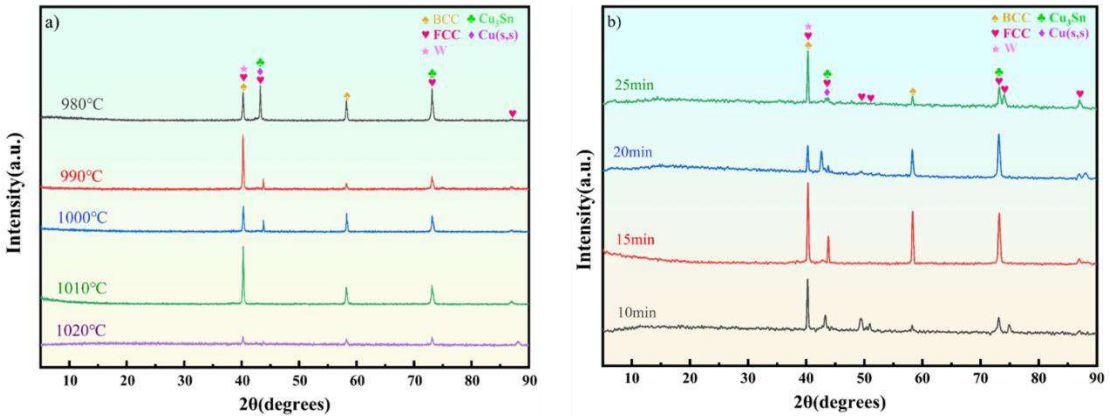


Fig. 6. XRD patterns of W/CuCrZr joints brazed with CoFeCrNiCuSn HEA filler: a) different brazing temperatures. b) different holding times.

Fig.7 shows the formation mechanism of CuCrZr/CoFeCrNiCuSn/W joint. The process of forming the joint was explained as follows. Initially, the process takes place at a temperature too low to melt the filler. Obviously, CuCrZr, filler and W are in close contact with each other, as illustrated in Fig. 7 a). Once the temperature is higher than the melting point, the liquid filler diffuses to both sides of CuCrZr and W. During this stage, Cu and Sn in the molten filler migrate toward the adjacent base materials and undergo elemental redistribution across the joint. The interaction between Cu and Sn promotes the formation of the Cu_3Sn intermetallic compound. According to the formula (1), the Gibbs free energy change for Cu_3Sn formation at 1000 °C is negative, indicating that the formation of Cu_3Sn is thermodynamically favorable under the brazing conditions.

$$3Cu + Sn \rightarrow Cu_3Sn \quad (1)$$

$$\Delta G_{Cu_3Sn}(kJ/mol) = -41.6kJ/mol - 5.96T = -34\ kJ/mol(1273K)$$

During the holding stage, Co, Fe, Cr and Ni form FCC phase under high- entropy effect [23-26]. At the same time, Cr, Co and Fe atoms continue to diffuse to the W side to form a W-Cr-based BCC phase (Fig. 7 d) [27, 28]. Cu and Sn form Cu_3Sn IMC. During the later stage of cooling, because the CoFeCrNiCuSn alloy is mainly composed

of copper-rich phase and copper-poor phase, Cu (s, s) phase is formed at the joint during the cooling process [29]. The microstructure of CuCrZr/W brazed with CoFeCrNiCuSn filler is shown in Fig. 7 e).

Fig. 8 shows the shear strength of joints varies under different process conditions. In both cases, increasing the temperature or prolonging the holding time will cause the shear strength to increase first and then decrease. The maximum shear strength of 247 MPa for the joint is attained at 1000 °C and 20 minutes, highlighting the best conditions for brazing. The fracture surfaces of the joints brazed at different temperatures were characterized using a 3D non-contact profilometer to investigate their surface morphology and fracture characteristics. Fig. 9 shows the fracture morphologies and fracture paths of the brazed joints obtained at different holding times. As the holding time increases, the joint fractures differently. With a holding time of 10 minutes, the main area of the fracture is relatively flat, and the local fluctuation is mainly distributed in the edge area, indicating that the wetting and the diffusion at the interface between the filler and base metal are insufficient, leading to a joint shear strength of only 177 MPa. As the holding time is extended to 15 min, the edge of the fracture shows obvious high ups and downs, and the maximum height reaches 1058.4 μm, indicating that the interface bonding is improved, and the strength of the joint reaches 198 MPa. However, the high fluctuation area of this group of fractures is mainly concentrated at the edge, and the central area is still relatively flat, indicating that the bonding uniformity of the effective connection area of the joint has not yet reached the best. When the holding time is further extended to 20 min, the shear strength of the joint reaches the maximum

of 247 MPa. At this time, the fracture surface presents a more continuous and uniform undulating morphology, indicating that the diffusion reaction between the filler and CuCrZr and W is more extensive, and the interface metallurgical bonding is enhanced. Therefore, 20 min is the optimal holding time of the system. It should be pointed out that the maximum height of the fracture is not the only factor determining the strength of the joint. Although the fracture surface of the joint brazed for 15 min exhibits the largest local height variation, the pronounced surface relief is mainly concentrated near the edges. In contrast, the fracture surface of the joint brazed for 20 min displays a more uniform overall morphology, suggesting a more uniform load-bearing behavior and improved interfacial bonding. Extending the holding time to 25 minutes leads to a significant decrease in shear strength to 143 MPa. The maximum height of the fracture also decreases to 409.9 μm, and the main area of the fracture tends to be flat, indicating that the plastic deformation and tearing degree during the fracture process are weakened. An excessively long holding time may promote excessive interfacial reactions and unfavorable microstructural evolution within the brazed seam, thereby facilitating crack propagation and reducing the shear strength of the joint. In addition, previous studies have shown that prolonged exposure of CuCrZr to elevated temperatures can cause partial dissolution and coarsening of strengthening precipitates as well as grain growth, resulting in softening of the alloy [30-32]. These results indicate that a moderate increase in holding time promotes the metallurgical bonding between CoFeCrNiCuSn filler and base metal, but too long holding time will cause excessive interface reaction and microstructure deterioration, and ultimately weaken the mechanical properties of

the joint.

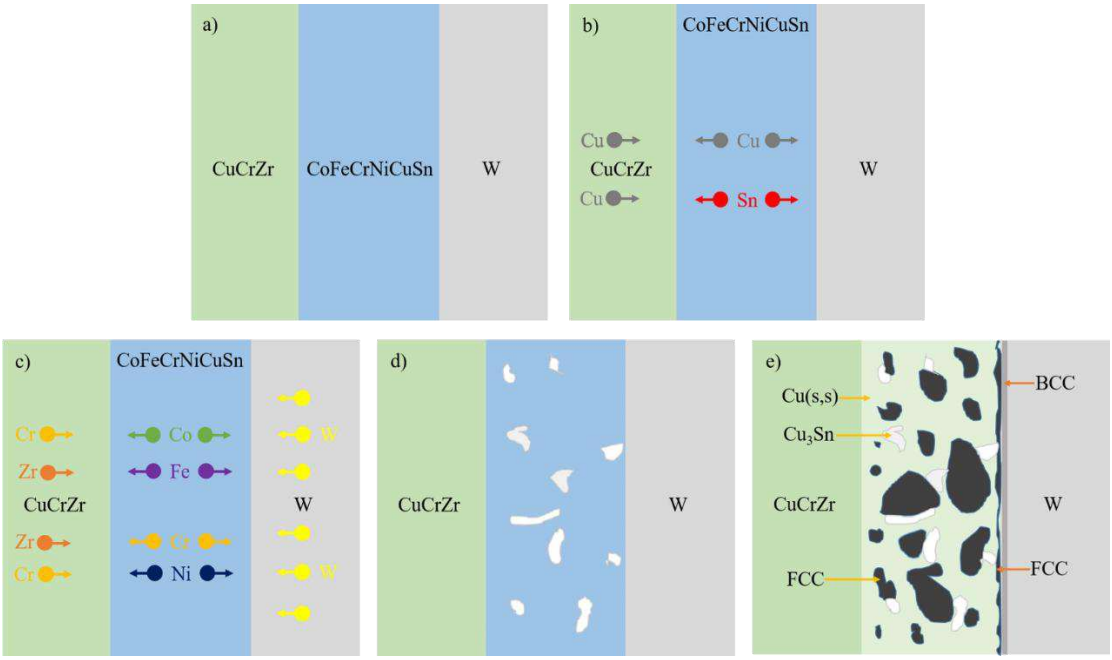


Fig. 7. Formation mechanism of brazed joint

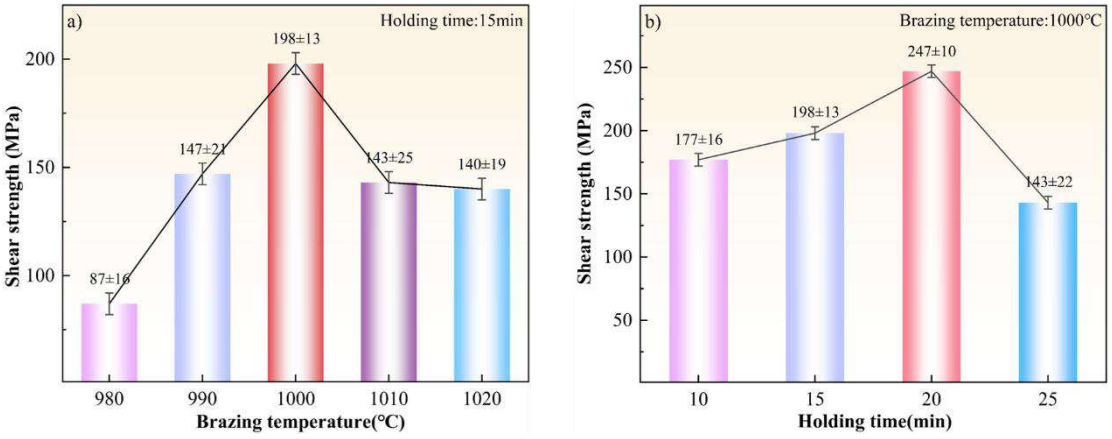


Fig. 8. Shear strength of the CuCrZr/CoFeCrNiCuSn/W joints brazed: a) different temperatures for 15 min. b) different holding times for 1000 ℃

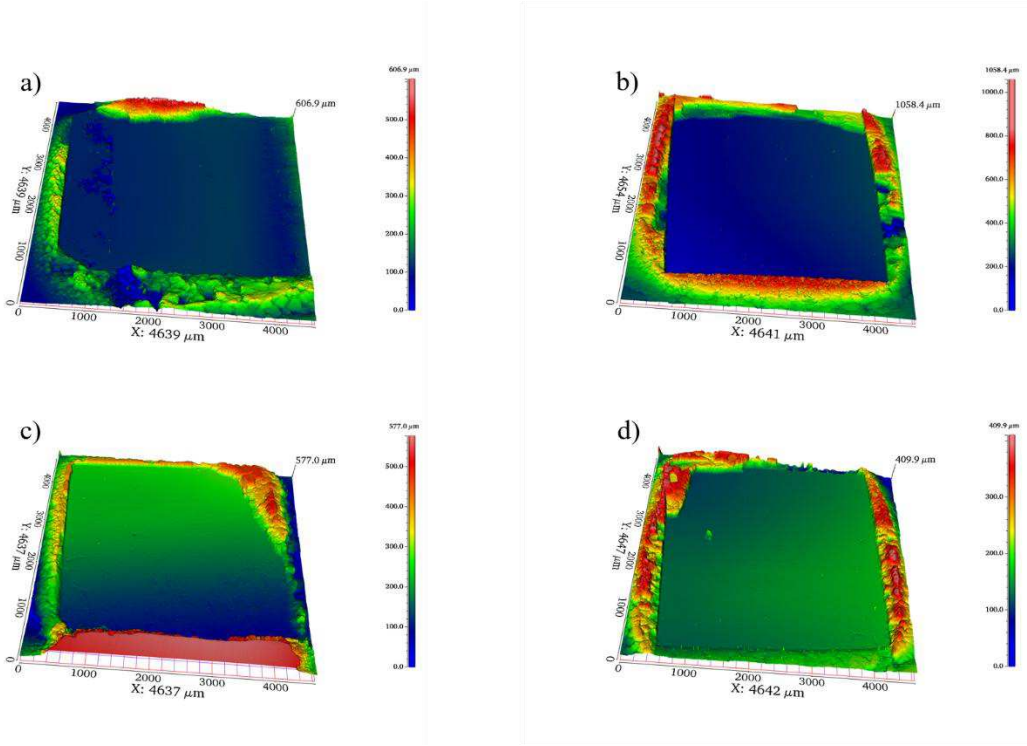


Fig. 9. Fracture 3D morphology of the CuCrZr/CoFeCrNiCuSn/W joints brazed at 1000℃ with different holding times: a) 10 min, b) 15 min, c) 20min and d) 25 min.

Fig. 10 shows the fracture morphology of CuCrZr side when the brazing process is 1000 °C/20 min. At 1000 °C for 20 min, the fracture surface on the CuCrZr side remains relatively intact, with a comparatively flat central region and distinct layered and blocky residual features near the edges. These features suggest that the molten filler metal exhibited good spreading and filling behavior along the CuCrZr interface during brazing. The high-magnification fracture morphology shows that the region ζ region is composed of a flat area, a rough area and a block reaction product, and typical dimples are not observed, indicating that the whole joint is dominated by brittle fracture. The EDS results in Table 2 show that position 1 is mainly enriched in Cu and Sn, which is speculated to be Cu_3Sn. Positions 2 and 4 are mainly composed of Cu, which is Cu (s, s). The elements at position 3 are mainly W and Cr, which are presumed to be W/Cr-rich BCC phases. For 20 min, the brittle Cu_3Sn intermetallic compound (IMC) is

distributed discontinuously within the joint, without forming a continuous brittle path for crack propagation. Such a distribution may provide local strengthening while limiting rapid crack propagation through the joint. Therefore, the 1000 °C/20 min joint exhibits the maximum shear strength.

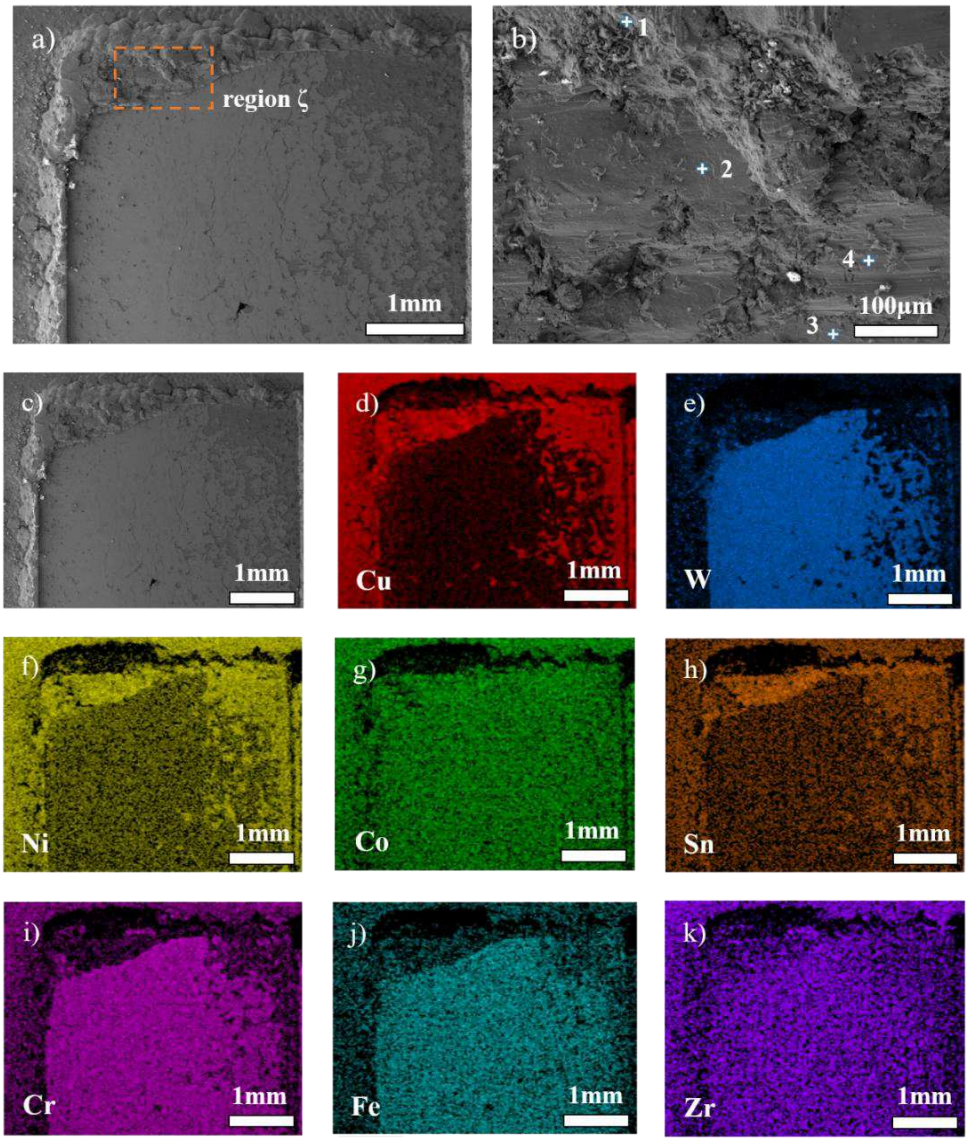


Fig. 10. Microstructure and element mappings of CuCrZr side shear fracture of brazing joint at 1000 ℃/20 min.

Table 2 Elemental compositions and possible phases in regions 1-4 in Fig. 10 (at.%).

Position	Cr	Fe	Co	Ni	Cu	Zr	Sn	W	Possible Phase
1	0.21	0.49	0.41	6.78	74.82	0.09	16.08	1.17	Cu_3Sn
2	0.32	0.28	0.09	1.66	93.37	0.16	3.93	0.18	Cu(s, s)
3	23.22	13.41	15.20	5.70	5.42	0.61	0.68	35.75	BCC
4	0.52	0.76	0.54	4.23	84.97	0.00	8.76	0.24	Cu(s, s)

The relative fractions of the FCC and Cu_3Sn phases play an important role in determining the shear strength of the brazed joint. FCC has good toughness and bearing capacity [33-35]. Cu_3Sn is an IMC formed by Cu-Sn reaction, which has high hardness but poor plasticity. Its influence on the joint is strongly dependent on its amount and spatial distribution. A limited amount of discontinuously distributed Cu_3Sn may contribute to local strengthening, whereas excessive or continuous Cu_3Sn can provide preferential sites and pathways for crack initiation and propagation [36-39].Fig. 11 a) - e) show the microstructure of the temperature group joint. Fig. 13 a) analyzes the volume fraction changes of FCC and Cu_3Sn phases in the joints of the temperature group. As shown in Fig. 13 a), at different brazing temperatures, the volume fraction of Cu_3Sn in the joint at 980 °C is as high as 22.24 %, while the FCC phase is only 77.76 %. The proportion of brittle phase in the weld is high, which leads to the rapid expansion of cracks along the Cu_3Sn phase interface, so the shear strength is only 87 MPa [37, 40]. With the increase of temperature to 1000 °C, the volume fraction of FCC phase increases to 92.86%, and Cu_3Sn decreases to 7.14%, forming a multiphase structure with FCC as the main body and a small amount of Cu_3Sn discrete distribution. Meanwhile, the brazed-seam width reaches 324 μm, accompanied by improved metallurgical bonding at the interfaces. These microstructural characteristics are

consistent with the increase in shear strength to 198 MPa. When the temperature is further increased to 1010 °C, the Cu_3Sn content increases to 13.63 %, and the brittle phase is coarsened or continuous, resulting in a decrease in joint strength. At 1020 °C, although the fraction of the FCC phase increases to 98.38% and that of Cu_3Sn decreases to 1.62%, the joint width decreases to 239 μm. The elevated brazing temperature may promote excessive elemental redistribution and interfacial reactions, leading to an unfavorable evolution of the brazed-seam microstructure. These changes may compromise the integrity of the joint and therefore prevent a further increase in shear strength.

The microstructure of the joints for the holding time group is shown in Fig. 12 a) - d). Fig. 13 b) analyzes the volume fraction changes of Cu_3Sn and FCC phases in these joints of the holding time group. For holding times of 10, 15, and 20 min, the volume fraction of the FCC phase remains at approximately 93%, while that of Cu_3Sn remains within the range of 6%-7%. These results indicate that the brazed seam is dominated by the FCC phase, with only a small fraction of Cu_3Sn present. Extending the holding time to 20 minutes, the joint width increases to 402 μm, and the interface reaction and element diffusion reach a better state. Therefore, the joint exhibits a maximum shear strength of 247 MPa. Extending the holding time to 25 minutes, the proportion of FCC phase increases to 96.81 %, Cu_3Sn decreases to 3.19 %, but the joint width shrinks to 208 μm. This shows that too long holding time will lead to excessive diffusion of low melting point components including Sn and Cu into base metals, reducing the effective connection area, and ultimately leading to a decrease in the shear strength of the joint

to 143 MPa [41]. Therefore, the joint strength depends on the proportion and distribution of FCC and Cu_3Sn.

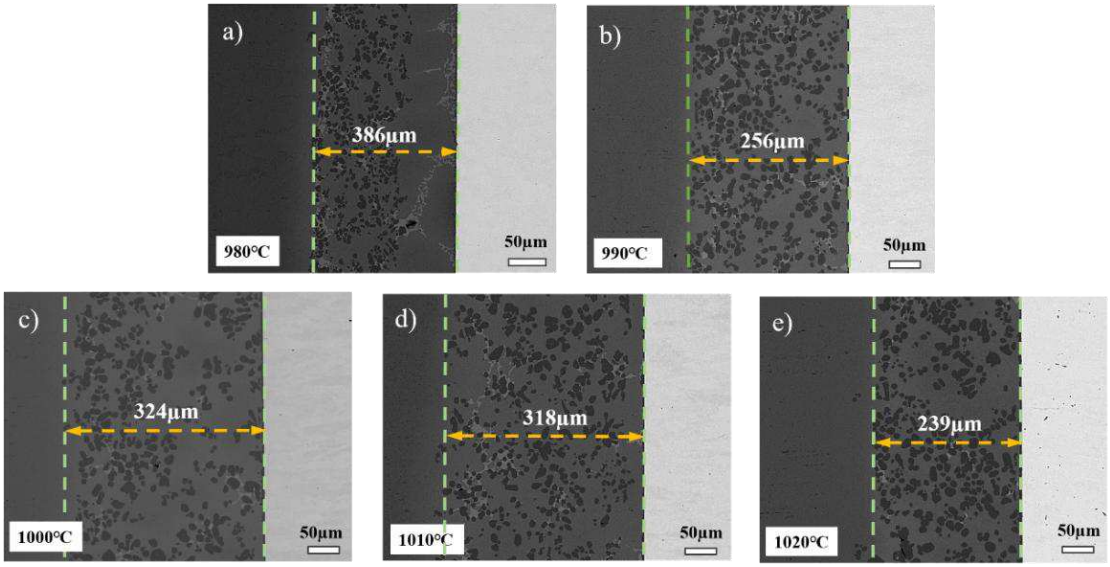


Fig. 11. Microstructure joints a) 980 °C; b) 990 °C; c) 1000 °C; d) 1010 °C; e) 1020 °C; f) volume fraction of FCC and Cu_3Sn phases with varying temperatures (holding time: 15 minutes).

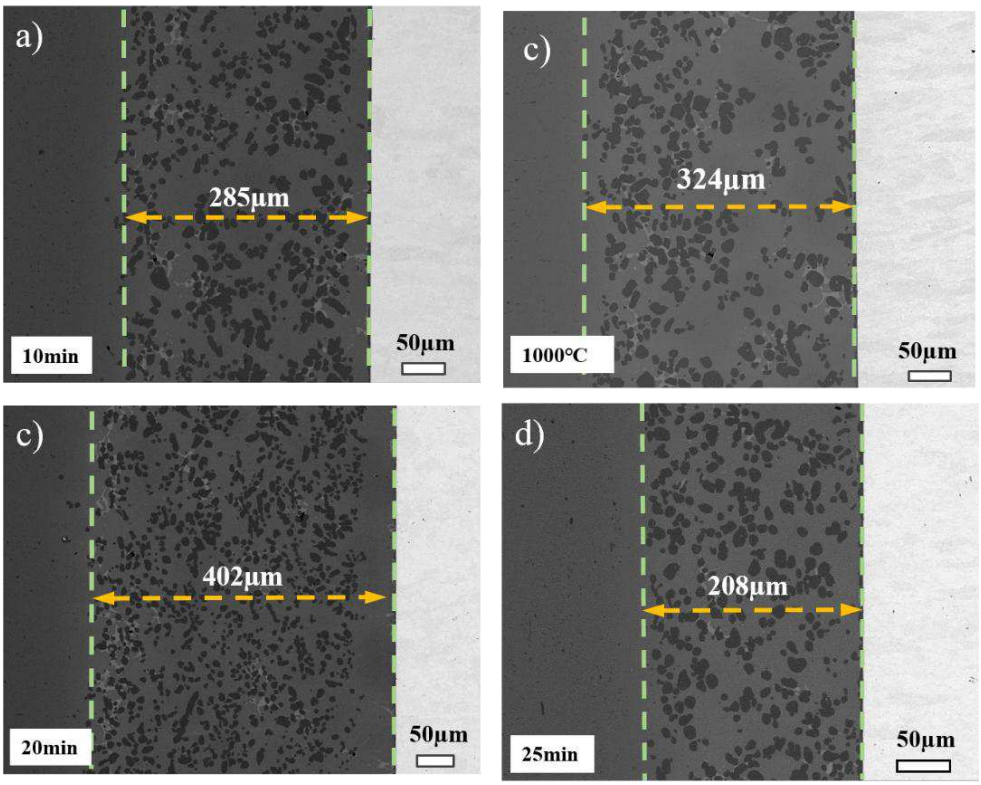


Fig. 12. Microstructure joints a) 10 min; b) 15 min; c) 20 min; d) 25 min; e) evolution of FCC and Cu_3Sn phases volume fractions with holding time at 1000 °C

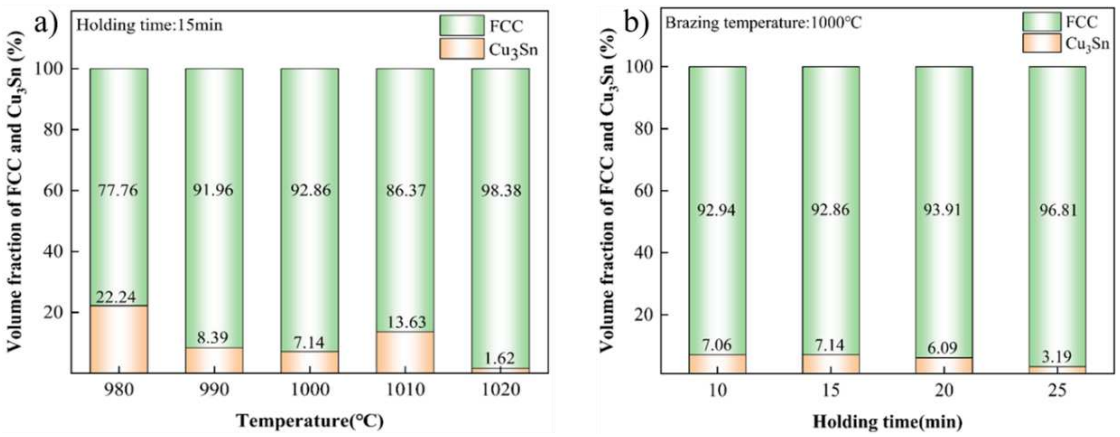


Fig. 13. a) volume fraction of FCC and Cu_3Sn phases with varying temperatures (holding time: 15 minutes); b) evolution of FCC and Cu_3Sn phases volume fractions with holding time at 1000 °C.

4. Conclusions

In this experiment, the vacuum brazing of CuCrZr and W is successfully carried out by using CoFeCrNiCuSn high-entropy filler. The study examines how holding time and brazing temperature influence the mechanical properties and microstructure of the joints. The primary conclusions are as follows.

1) CuCrZr and W are successfully joined by brazing using a CoFeCrNiCuSn high-entropy alloy filler. The brazed joint is mainly composed of FCC, W-rich BCC, Cu-based solid-solution, and Cu_3Sn phases, with the FCC phase constituting the dominant matrix. A limited amount of discontinuously distributed Cu_3Sn may contribute to local strengthening without forming a continuous brittle path for crack propagation, whereas excessive or continuous Cu_3Sn can facilitate brittle fracture.

2) The brazing temperature and holding time affect the strength of the joint. With the increase of temperature and time, the interface diffusion and metallurgical bonding are enhanced, and the joint strength increases first and then decreases.

3) At 1000 °C/20 min, the proportion of each phase is reasonable, and the shear strength reaches the maximum of 247 MPa. Further increasing the temperature or holding time will lead to excessive diffusion of Cu and Sn, causing joint strength to decline. The joint fracture is identified as a brittle fracture.

Declaration of competing interest

The authors declare that they have no known competing financial interests or personal relationships that could have appeared to influence the work reported in this paper.

Author contributions

Writing-Original draft preparation: Rui Zhang; Data curation: Rui Zhang, Yinhe Zeng; Writing-Reviewing and Editing: Gang Wang; Visualization and Investigation: Wei Wang; Data processing and Validation: Yu Zhao; Supervision: Rujie He and Caiwang Tan.

Acknowledgement

This work was financially supported by the National Natural Science Foundation of China [52171148], The University Synergy Innovation Program of Anhui Province [GXXT-2023-025; GXXT-2023-026], Anhui Provincial University Innovation Team [2025AHGXZK10039], Science and Technology Research Project of Anhui Provincial [202423i08050011], 2024 Discipline (professional) Leader Training program of Anhui Provincial Department of Education [No. DTR2024099].

References

[1] E. Pakhomova, A. Palombi, A. Varone, Plasma Spraying of W Coatings for Nuclear Fusion Applications: Advancements and Challenges, Crystals, 15 (2025).

[2] D.H. Zhu, J.L. Chen, Z.J. Zhou, R. Yan, Thermal-mechanical analysis on W/CuCrZr plasma facing component with functionally graded material interlayer, Journal of Physics: Conference Series, 419 (2013) 012038.

[3] M. Zarinejad, Y. Tong, M. Salehi, C. Mu, N. Wang, Y. Xu, S. Rimaz, L. Tian, K.X. Kuah, X. Chen, Advancements and Perspectives in Additive Manufacturing of Tungsten Alloys and Composites: Challenges and Solutions, Crystals, (2024).

[4] J. Li, Z. Kuai, Z. Li, B. Liu, Y. Chen, S. Lu, Y. Nie, Z. Yang, Effects of Process Parameters on the Relative Density and Properties of CuCrZr Alloy Produced by Selective Laser Melting, Metals (2075-4701), 12 (2022).

[5] J. Cao, J.W. Gao, W.D. Zhao, P.P. Xue, B. Yang, C. Li, J.L. Qi, X.Q. Si, Research Progress on Brazing of Dissimilar Metals, Acta Metallurgica Sinica, 62 (2026) 117-132.

[6] L. Han, J. Wang, Y. Chen, Z. Liu, Y. Huang, D. Liu, L. Luo, C. Liu, Y. Liu, Z. Wang, Diffusion bonding and interface structure of advanced carbide-dispersion-strengthened Cu and oxide-dispersion-strengthened W, Journal of Materials Processing Technology, (2022) 302.

[7] Y.-Y. Chen, Z. Liu, S.R. Meka, Y. Huang, Z.-M. Wang, Effect of interface structure on advanced bonding between tungsten-based materials and Cu alloys: a review, 7 (2025) 479-496.

[8] J. de Prado, M. Sánchez, I. Izaguirre, D. Swan, A. Ureña, Exploring Cu-Ge alloys as filler materials for high vacuum brazing application of W and CuCrZr, Materials Today Communications, 33 (2022) 104286.

[9] W. Zhou, G. Chen, H. Pan, F. Luo, Y. Wei, M. Li, Laser precision profiling of small-angle bevel-edge contour grinding wheels, Journal of Materials Processing Technology, 305 (2022) 117591.

[10] YiZhou, ChunzhiXia, JunYang, XiangpingXu, JiashengZou, Microstructure and properties of W-Cu/1Cr18Ni9 steel brazed joint with different Ni-based filler metals,

Science & Engineering of Composite Materials, (2018).
[11] YiZhou, ChunzhiXia, JunYang, XiangpingXu, JiashengZou, Investigation of the microstructure and properties of W75-Cu/W55-Cu brazed joint with Cu-Mn-Co filler metal, Science and Engineering of Composite Materials, 25 (2018) 17-23.
[12] Y. Zhang, W. Guo, H. Mei, X. Kong, Y. Zhu, X. Li, W. Zhao, H. Zhang, The novel high-entropy alloy filler realized the efficient inhibition of the violent reaction and brittle phase formation in the SiCf/SiC heterogeneous brazed joint, Materials Characterization, 222 (2025).
[13] K. Furkan, R.S. Harini, J.J. Pil, Recent Advances in High Entropy Alloy Fillers for Brazing Similar and Dissimilar Materials: A Review, Metals and Materials International, 30 (2024) 1145-1169.
[14] Z. Luo, G. Wang, Y. Zhao, C. Tan, R. He, Brazing SiC ceramics and Zr with CoCrFeNiCuSn high entropy alloy, CERAMICS INTERNATIONAL, (2022) 48.
[15] G.W. A, Y.Y. A, M.W. A, R.H. B, C.T. C, W.C. D, H.F.X. E, Brazing ZrB2-SiC ceramics to Nb with a novel CoFeNiCrCu high entropy alloy - ScienceDirect, Journal of the European Ceramic Society, 41 (2021) 54-61.
[16] S. Li, X.N. Hou, X. Wang, Z. Liu, Y. Xia, H. Dong, Weldability of high entropy alloys: Microstructure, mechanical property, and corrosion resistance, Journal of Manufacturing Processes, (2023).
[17] D. Bridges, D. Fieser, J.J. Santiago, A. Hu, Novel Frontiers in High-Entropy Alloys, Metals, 13 (2023) 22.
[18] S. Meng, M. Zhang, Y. Han, W. Liu, Y. Ma, Q. Cai, Effect of bonding time on the interfacial microstructure and mechanical properties of diffusion bonded tungsten alloy/steel joints using CrFeCoNiCu high entropy alloy interlayer, Journal of Materials Research and Technology, 33 (2024) 9386-9393.
[19] L.A. Thi Nguyen, S. Lee, S.J. Noh, S.K. Lee, M.C. Park, W. Shu, S. Pitcher, T. David, G. David, J. Kim, Desorption dynamics of deuterium in CuCrZr alloy, Journal of Nuclear Materials, (2017) S0022311517307304.
[20] L. Huang, X. Wang, B. Huang, X. Zhao, H. Chen, C. Wang, Effect of Cu segregation on the phase transformation and properties of AlCrFeNiTiCux high-entropy

alloys, Intermetallics, (2022) 140.
[21] D.-G. Liu, J.-X. Zou, H. Liu, Z.-Q. Li, S.-S. Chang, L. Zheng, L.-M. Luo, C.-F. Hong, Microstructure, mechanical properties and hermeticity of W-Cu/HTCC brazed joints with surface metallization, International Journal of Refractory Metals and Hard Materials, 118 (2024) 106473.
[22] T. He, Y. Qi, Y. Ji, M. Feng, Grain boundary segregation-induced strengthening-weakening transition and its ideal maximum strength in nanopolycrystalline FeNiCrCoCu high-entropy alloys, International Journal of Mechanical Sciences, (2023).
[23] B. Chai, X. Fan, X. Wang, L. Fu, Microstructure and mechanical properties of the C/C composites and Nb joints brazed with CoCrFeNi HEAs, Science & Technology of Welding & Joining, 29 (2024) 447–455.
[24] Y. Lei, Y.N. Li, Y.C. Cai, X.Y. Wang, S.P. Hu, X.G. Song, Z.B. Chen, H.C. Shi, Vacuum brazing of Al0.3CoCrFeNi high-entropy alloys with CoCrFeNiNb0.5 eutectic filler metal for wide-temperature range application, Vacuum, 230 (2024).
[25] H.X. A, L.S. B, C.L. A, H.L. A, Y.H. A, W.C. A, Y.L. A, J.Y. A, W.Z. A, Y.M. A, A novel joining of C f /C composites using AlCoCrFeNi 2.1 high-entropy brazing filler alloys, Materials Characterization, 179 (2021).
[26] B. Wu, C. Song, M. Wang, F.X. Li, W. Yu, Brazing mechanism of Al0.1CoCrFeNi with composite structure nano-multilayer foils: Molecular dynamics and experimental perspectives, Intermetallics, 188 (2026) 109030.
[27] C. Wang, Z. Zhong, Y. Zhang, K. Song, P. Hua, A. Liu, Y. Wu, Interfacial microstructure evolution and mechanical behavior of W/steel joints diffusion bonded with CoCrFeNi interlayer, Materials Today Communications, 40 (2024) 109411.
[28] C. Wang, Z. Xiong, K. Song, C. Chen, K. Ling, Y. Wu, Z. Zhong, On the use of CoCrFeNi high entropy alloy as a new interlayer for achieving high strength diffusion bonded tungsten/steel joint, Materials Today Communications, 34 (2023) 105251.
[29] T. Nagase, T. Tamura, Solidification Microstructures in 3d-transition Metal High Entropy Alloys with Cu Element, Journal of Japan Institute of Copper, 60 (2021) 167-175.
[30] B. Shao, S. Zhao, P. Wang, X. Nai, H. Chen, Y. Liu, P. Wang, X. Song, W. Li,

Reaction mechanisms and mechanical properties of SiCf/SiC composite and GH536 superalloy joints using CoFeNiCrMn high-entropy alloy filler, Journal of Materials Research and Technology, 33 (2024) 12.

[31] X. Ren, H. Wang, W. Li, Q. Dong, B. Chen, W. Mao, Effect of holding time on interfacial evolution and mechanical strength of wide-gap brazed K417G superalloy joints, Welding in the World, 68 (2024) 3079-3084.

[32] I. Izaguirre, J. De Prado, N. Ordás, M. Sánchez, A. Urea, Brazeability Study of an Additively Manufactured CuCrZr Alloy to Tungsten Using Various Cu-Based Fillers, Materials (1996-1944), 18 (2025).

[33] E.P. George, W.A. Curtin, C.C. Tasan, High entropy alloys: A focused review of mechanical properties and deformation mechanisms, Acta Materialia, (2020).

[34] D.H. Chung, J. Lee, Q.F. He, Y.K. Kim, K.R. Lim, H.S. Kim, Y. Yang, Y.S. Na, Hetero-deformation promoted strengthening and toughening in BCC rich eutectic and near eutectic high entropy alloys, Journal of Materials Science & Technology, (2023) 1-9.

[35] Z. Guo, F. Zhou, J. Yu, J. Ding, E. Ma, Q. Yu, Phase Transformation‐Assisted Nucleation and Growth of a Single‐Phase FeCoNiCuNb Alloy, Advanced Science, 13 (2026).

[36] J. Zhang, Z.H. Jiang, Y. Zhang, Effect of Grain Structure on the Failure Mechanism of Cu/Cu3Sn Investigated Via Molecular Dynamic Simulations, (2022).

[37] J. Xie, L. Tang, L. Li, Z. Zhang, X. Ma, Interfacial reaction characteristics of Cu/Sn-0.3Ag-0.7Cu-xNi/Cu-soldered joints after isothermal aging, Journal of Materials Science: Materials in Electronics, 36 (2025) 1-13.

[38] Y.W. Wang, Effects of surface diffusion and solder volume on porous-type Cu3Sn in Cu/Sn/Cu microjoints, Materials Chemistry and Physics, 275 (2022) 125307.

[39] Yang, Chaoran, Le, Fuliang, Lee, S., W., Ricky, Experimental investigation of the failure mechanism of Cu-Sn intermetallic compounds in SAC solder joints, Microelectronics & Reliability, (2016).

[40] M.S. Luo, H.G. Wang, B. Chen, G.C. Lyu, X.P. Zhang, Finite Element Simulation Study of the Effects of Kirkendall Voids in IMC Layer on Interfacial Crack and

Reliability of Cu–Sn Solder Joint, 2023 24th International Conference on Electronic Packaging Technology (ICEPT), 2023, pp. 1-5.

[41] M.M. Sami, T. Zaharinie, F. Yusof, T. Ariga, Investigation on Strength and Microstructural Evolution of Porous Cu/Cu Brazed Joints Using Cu-Ni-Sn-P Filler, Metals - Open Access Metallurgy Journal, 10 (2020) 416.